Chapter 7

Generalized Results

This chapter analyzes the results of the pre-design procedures. The sensibility of the output to conveyor specifications and initial conditions is studied considering air-bearings in both carrying and return sides. Included is also an analysis of actual air-cushion conveyors, comparison with the model and flow simulation with ANSYS.

7.1 Results

With the purpose to generalize results, a model situation will be used. In table (7.1) the conveyor specifications for this purpose are listed.

Parameter	**Symbol**	**Units**	**Value**
Capacity	C	t/h	1000
Length	L	m	1000
Lift of the load	H	m	0 (!)
Velocity	U	m/s	3.5
Belt type	PN315/2	-	-
Conveying angle	α	$^\circ$	0 (!)
Belt width	B	m	1.000
Bulk material density	ρ_{bulk}	Kg/m^3	1000

Table 7.1: Conveyor Specifications

The results are tabulated for the situation were air-bearings are implemented in both sides (2S) and with return idlers(RI).

The results on power do not consider fans and drives efficiency nor losses in the supply system. Hp is the power demanded by the air-bearing and Hd the power necessary to maintain belt velocity. The real power should be corrected by a factor of about 1.6 for the pumping power (losses in the supply circuit and fans efficiency) and of about 1.1 for the drive power (drive system efficiency). It was not considered because it is dependent on the characteristics of the chosen fans and drives, and on the supply configuration. Presenting the results in this way is advantageous for posterior correction.

Table (7.4) contains the list of initial conditions.

The support material can be a carbon steel or a low alloy steel. For the present calculations only the yield strength is necessary. The safety factor on the yield strength and load were chosen taking in consideration typical values and suggestions from reference [5].

The scrapers pressure force and related friction coefficients were stipulated with reference [25].

The return side mass of moving parts was chosen with reference [10].

In doubt about the starting factor, since the drive mechanism is not yet specified, it was chosen as the maximum suggested in reference [26].

According to reference [2] the usual pressure ratio for hydrostatic bearings is $\beta = 0.5$. This value can handle an overload of almost 100 %. This may be exaggerated for the air-cushion conveyor. Specifying the overload to 50 % a pressure ratio of $\beta_r = 0.7$ will suffice. For the return side, the overload is null and the pressure ratio can be higher.

Belt properties were taken from reference [18] and air properties from reference [6].

Parameter	**Symbol**	**Units**	**2S**	**RI**
Pumping power	H_p	kW	16	15
Drive power	H_d	kW	8	17
Total power	H_t	kW	24	31
Total flow	Q_t	m^3/s	7	6
Take-up tension	T_2	kN	1.3	2.8
Working tension	T_{max}	kN	3.5	7.5
Carrying side temperature rise	$\triangle T_c$	$^\circ C$	2	2
Return side temperature rise	$\triangle T_r$	$^\circ C$	2	-
Belt arc	θ	$^\circ$	97	97
Support radius	r	m	0.59	0.59
Supply pressure	p_s	Pa	2300	2300
Carrying side support thickness	l_s	mm	2.6	2.6
Return side support thickness	l_{sret}	mm	0.8	-

Table 7.2: Results for the reference configuration and conditions

Property	**Symbol**	**Units**	**Value**
Viscosity	μ	Ns/m^2	1.8 $\times 10^{-5}$
Density	ρ	Kg/m^3	1.2
Specific heat	c_p	$W/Kg \cdot K$	1005

Table 7.3: Air properties at 20°

Parameter	**Symbol**	**Unit**	**Value**
Fluid thickness	h_c, h_r	mm	0.6
Distance between orifices	$\triangle x$	mm	50
Belt carcass thickness	t_{belt}	mm	2.7
Belt bottom cover thickness	t_{bc}	mm	1.0
Belt upper cover thickness	t_{uc}	mm	2.0
Belt density	ρ_{belt}	kg/m^3	1386
Carrying side pressure ratio	β_c	-	0.7
Return side pressure ratio	β_r	-	0.8
Support material yield strength	S_y	MPa	240
Safety factor on material strength	n_s	-	1.2
Safety factor on load	n_l	-	1.2
Drive pulley friction factor	μ_p	-	0.35
Drive pulley angle of contact	θ_p	$^\circ$	230
Starting factor	f_{start}	-	1.8
Friction factor	f_e	-	0.02
Ret. side mass of moving parts	Q	Kg/m	13.6
Secondary scraper friction coefficient	μ_{scr2}	-	0.75
Secondary scraper normal force	F_{scr2}	N/m	800
Primary scraper friction coefficient	μ_{scr1}	-	1.00
Primary scraper normal force	F_{scr1}	N/m	400

Table 7.4: Initial conditions

7.2 Influence of Specifications and Initial Parameters on Results

In this section the influence of parameters as length, capacity, belt with, conveying angle, temperature and fluid thickness will be analyzed. What is pretended is the influence of these parameters on the results of the pre-design procedures.

Both carrying and return sides are supported by air-bearings.

If some initial conditions change, how does this affect the results?...

7.2.1 Influence of Conveyor Length

The length has influence on the flow, power requirements, working and take-up tensions.

Influence of Conveyor Length on Power Requirements and Flow

The required power per meter decreases with conveyor length. The flow is proportional.

In figure (7.1), by linear regression the total power has a behavior given by $H_t[kW] = 17 \times L[km] + 7$. The total power per km becomes lower for higher lengths. The constant component has to do with the losses on the scrapers and the force to accelerate the bulk material.

For long lengths the major contributor for the total power is the pumping power, while the drive power is kept relatively low. We have $H_d[kW] \approx 0.7 \times L[km] + 7$ and $H_p[kW] \approx 16.3 \times L[km]$. Having constant supply pressure, the pumping power only depends on the flow, which grows linearly: $Q_t[m^3/s] = 7 \times L[km]$

Influence of Conveyor Length on Working and Take-Up Tensions

For long length conveyors the working and take-up tensions are still relatively low.

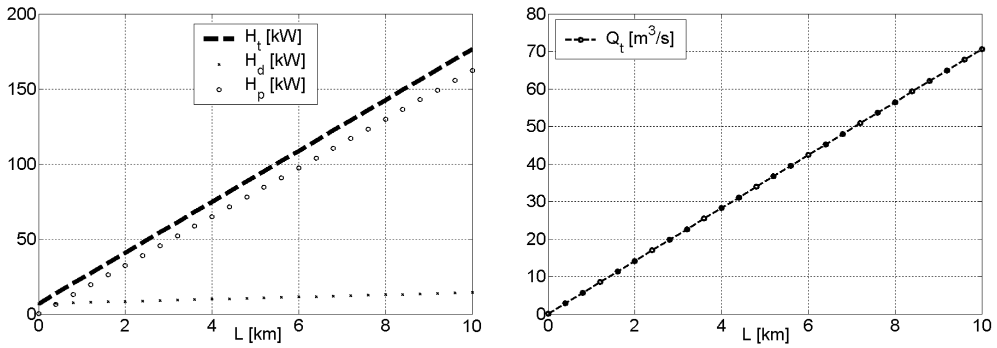

Figure 7.1: Power vs conveyor length

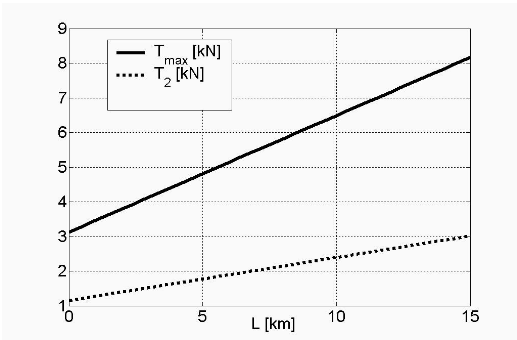

Figure 7.2: Working and take-up tensions vs conveyor length

The influence of the length on belt tensions is linear. The working tension is $T_{max}[kN] = 0.34 \times L[km] + 3.1$ and the take-up tension $T_2[kN] = 0.12 \times L[km] + 1.2$.

For the considered PN315/2 belt and the length range $L[km] < 15$ the safety factor is still on the recommended limit ($sf \geq 10$). For $L[km] = 15$ it has the minimum value, $sf = 19.7$, and should be considered over-designed. Though, this belt was the one of lower resistance in the chosen catalog [10].

7.2.2 Influence of Velocity

The velocity has influence on several parameters: temperature rise, tensions, pumping and drive power, and geometric parameters.

Influence of Velocity on Working and Take-Up Tensions

Increasing velocity will increase both working and take-up tensions.

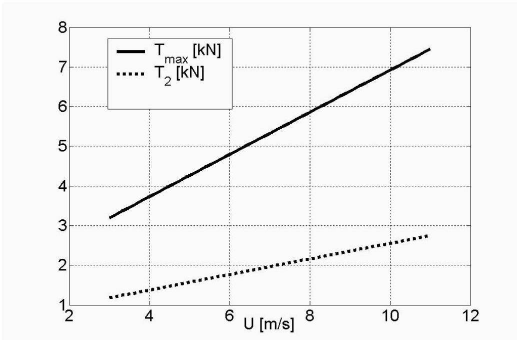

Figure 7.3: Working and take-up tensions vs velocity

Both working and take-up tensions grow proportionally to the velocity, as the viscous drag force and the bulk acceleration force are proportional to the velocity. The working tension is $T_{max}[kN] = 0.53 \times U[m/s] + 1.6$ and the take-up tension $T_2 = 0.2 \times U[m/s] + 0.6$.

Influence of Velocity on Power Requirements and Flow

Higher velocities require less flow and less pumping power, but the drive power increases.

As velocity is increased the load pressure decreases and this is reflected in the required flow and pumping power.

The drive power increases with velocity mostly because of scrapers resistance and bulk material acceleration.

If the velocity is fixed at $U[m/s] = 4.5$ instead of $U[m/s] = 3.5$, the total power H_t is minimum and has a reduction of 10% and the flow Q_t a reduction of 18%.

Influence of Velocity on Geometric Parameters

Increasing velocity is favorable to reduce support thickness.

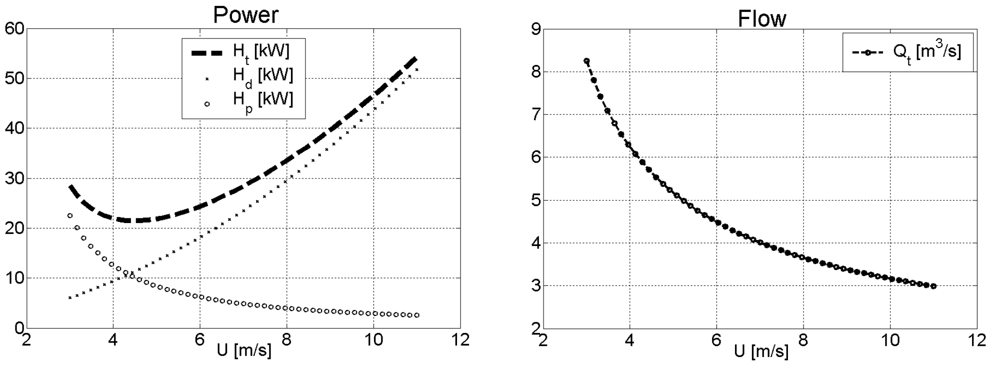

Figure 7.4: Power and Flow vs Velocity

Having a fixed capacity, increasing the velocity the pre-design procedures lead to a lower belt arc radius. This is due to the reduction of bulk area. The support tends to be flat.

The most relevant benefit of velocity increasement is on the reduction of the carrying side support thickness (further referred simply as support thickness)

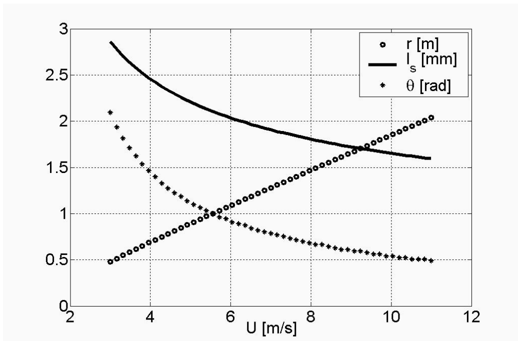

Figure 7.5: Support thickness, radius and belt arc vs velocity

Influence of Velocity on Temperature Rise

Effects on temperature rise are significant for small fluid thickness.

The influence of velocity on temperature rise is not significant in the range

$3 < U[m/s] < 11$. The behavior is not linear, but in absolute there is a difference of $5°C$.

The reference fluid thickness is $h_c = h_r = 0.6mm$. With smaller fluid thickness the effect would be more significant. For $h_r = 0.3mm$ and $U = 11m/s$, the temperature rise would be around $100°C$.

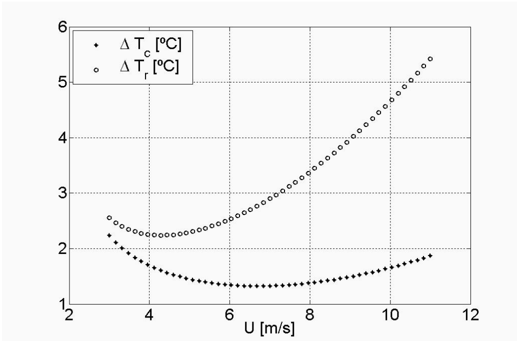

Figure 7.6: Temperature rise vs velocity

7.2.3 Influence of Reference Temperature

Temperature has influence on air viscosity and density. For higher temperatures air has lower density and higher viscosity. This will affect the flow, power requirements, temperature rise and tensions.

As an important note, it should be regarded that what is presented in this subsection is not the influence of ambient temperature variations on a build air-cushion conveyor, but the influence on the pre-design results of the temperature at which the air-properties are specified, the reference temperature. This analysis is carried out to check the sensibility of the results to the reference temperature.

Influence of Reference Temperature on Power Requirements and Flow

Higher reference temperatures lead to lower power and flow requirements.

For lower reference temperatures the results on power requirements and flow

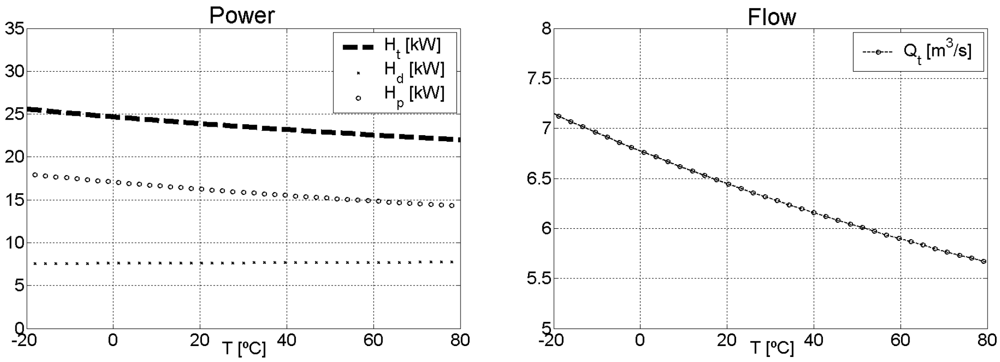

Figure 7.7: Power and flow vs reference temperature

are higher. The pumping power is more affected by the reference temperature, while the drive power remains practically constant.

Influence of Reference Temperature on Take-Up and Working Tensions

Reference temperature does not have significant influence on belt tensions.

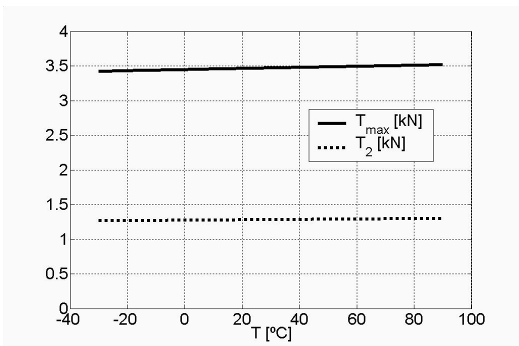

Figure 7.8: Take-up and working tensions vs reference temperature

In what concerns the resistance forces on the belt, the temperature has direct influence on the viscous drag forces F_c and F_r; but because of the relatively low value these forces have, temperature effect on the overall resistance is modest.

For the range of reference temperatures $-30 < [°C] < 90$ the working tension

T_{max} and the take-up tension T_2 have an absolute variation of 3%.

Influence of Reference Temperature on Temperature Rise

The reference temperature has a modest effect on temperature rise.

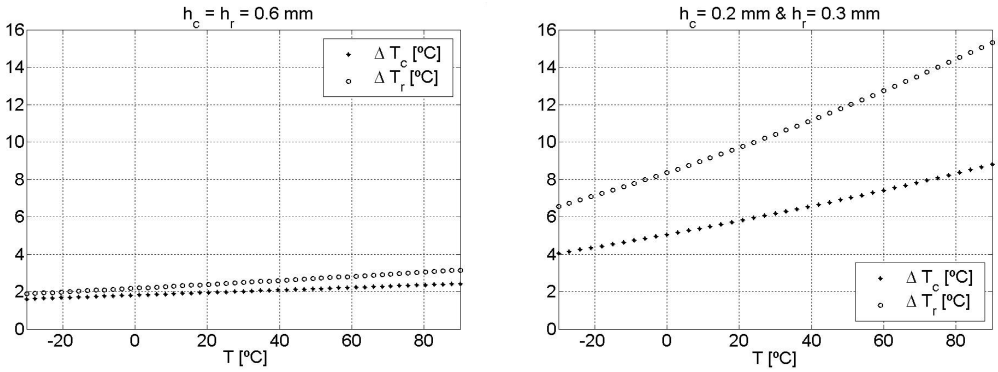

Figure 7.9: Temperature rise vs reference temperature

For the actual configuration the effects of the reference temperature on the rise of carrying and return sides fluid temperature is of about $1°C$ in the the range $-30 < [°C] < 90$.

For lower fluid thickness the effects of reference temperature on temperature rise would be more noticeable. The behavior is almost linear and for higher reference temperatures the temperature rise effect is aggravated.

7.2.4 Influence of Lift or Fall of the Load

The height of lift or fall of the load H has influence on drive power and on belt tensions. The remaining parameters are unaffected.

Influence of Lift or Fall of the Load on Power and Tensions

Tensions and power requirements increase with increasing lift of the load. With fall of the load, the regenerative mode starts for low inclines.

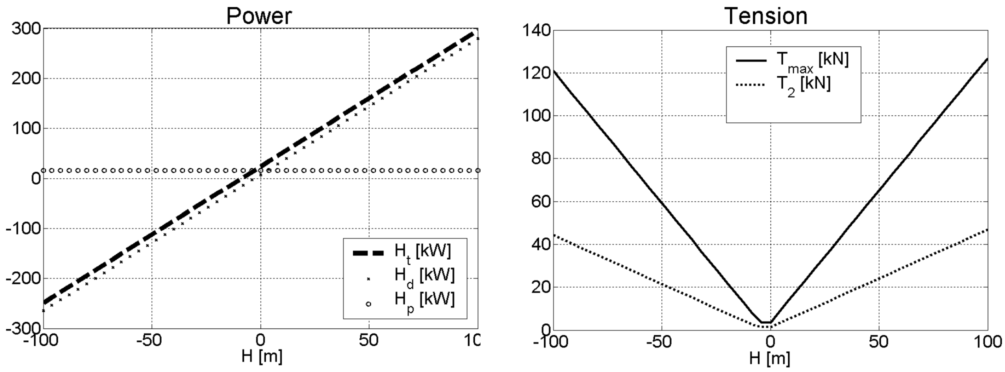

Figure 7.10: Power and tensions vs lift or fall of the load

The fall of the load has advantages to the drive power, as the conveyor works in the regenerative mode. The pumping power is not affected.

The total power is $H_t[kW] = 2.7 \times H[m] + 24$. The regenerative mode occurs for $H[m] < -3$. For $H[m] < 9$ the regenerated drive power is enough to supply the pumps (not accounting for efficiency on drives and fans).

For $H[m] < -1$ the take up-tension is specified to avoid negative tensions on the belt, and for $H[m] > -1$ it is based on the the rope friction law.

The working tension has an accentuated slope for $H > 0$ because the gravity forces on the load act on the direction of the main resistances.

The safety factor $sf \geq 10$ for the PN315/2 belt is respected in the range $-14 < H[m] < 11$.

7.2.5 Influence of Capacity

Capacity has influence on all relevant parameters.

The allowed capacity depends on the belt width and on the velocity. For low width belts and low velocities the capacity is limited by the belt arc angle, that it is supposed to be $\theta < 180°$. For this reason the graphics are limited in the capacity range.

Influence of Capacity on Power and Flow

Increasing capacity increase power requirements and flow.

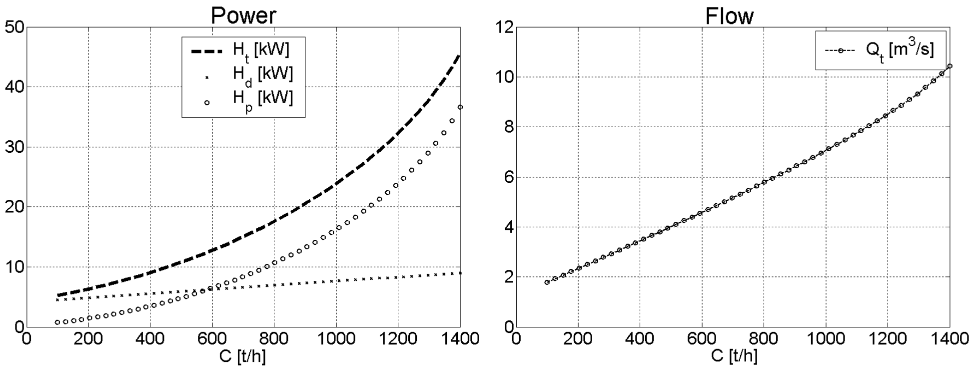

Figure 7.11: Power and flow vs capacity

With decrease in capacity both power and flow decrease. While the flow has a linear behavior with capacity, for the pumping power the curve is quadratic, because the necessary supply pressure also decrease.

Influence of Capacity on Tensions

An increase in capacity increase belt tensions. The behaviour is not linear.

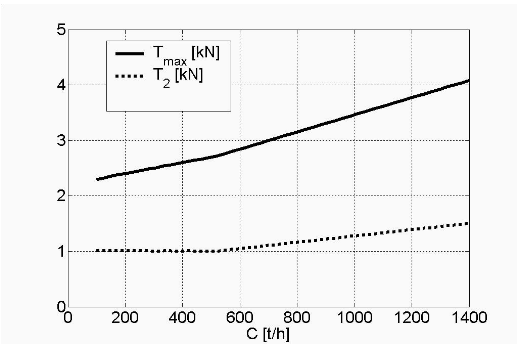

Figure 7.12: Take-up and working tensions vs capacity

It was expected that tensions on the belt decrease with decrease in capacity. Though the relation is not linear. For $C[t/h] < 500$ the take-up tension T_2 is determined to avoid negative tensions. For $500 < C[t/h] < 1100$ it is derived from the rope friction law.

The working tension T_{max} is the tight side tension on the drive pulley T_1.

Influence of Capacity on Geometric Parameters

Increasing capacity requires a thicker support with a smaller radius.

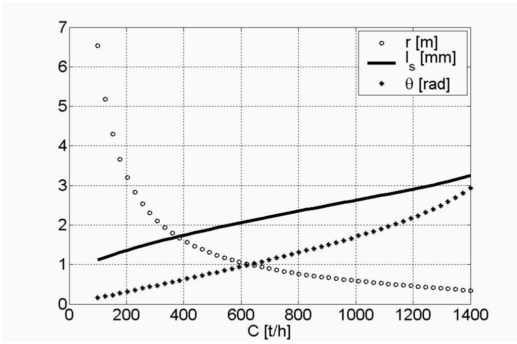

Figure 7.13: Support radius and thickness, belt arc angle vs capacity

Increasing capacity tends to increase the support thickness - as a direct result from the increase in supply pressure - and the belt arc angle, because the bulk i bigger.

Influence of Capacity on Temperature Rise

The effects of capacity on temperature rise are important just with small fluid thickness.

The temperature rise behavior with capacity is non-linear; it can both increase or decrease with increase in capacity. The dependence with fluid thickness is to take into consideration.

For the actual configuration the temperature rise grows with capacity. In the range $100 < C[t/h] < 1400$ the extreme values differ less than $3°C$.

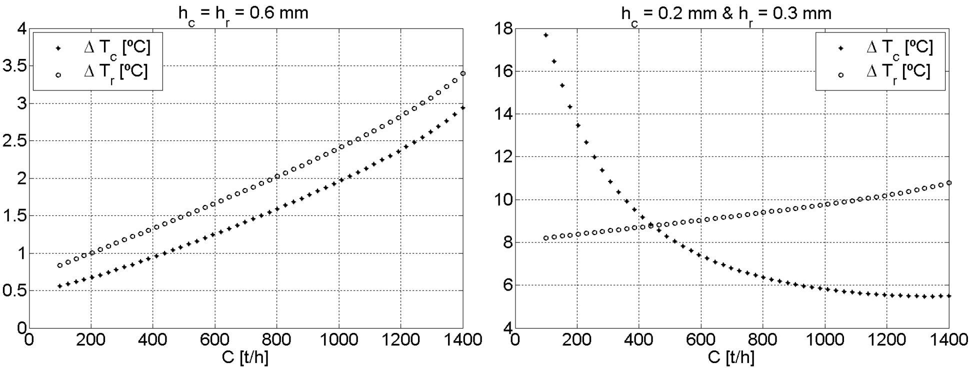

Figure 7.14: Temperature rise vs capacity

7.2.6 Influence of Bulk Density

Bulk material density has mainly influence on flow, power consumption and geometric parameters. The effects on temperature rise are low and on tensions are none.

Influence of Bulk Density on Geometric Parameters

The required support radius decrease with increase in bulk material density.

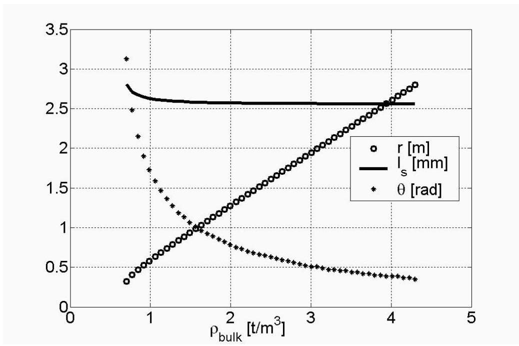

Figure 7.15: Support thickness and radius, belt arc angle vs bulk density

Smaller density bulk materials lead to increase the belt arc angle, for fixed velocity, capacity and belt width. This is due to the increase in bulk area. The opposite, for higher densities, may be a problem if the belt arc angle is too low. Changing the velocity or the belt width is a possible solution.

The necessary support thickness does not change significantly.

Influence of Bulk Density on Power and Flow

Power consumption and flow are only slightly affected by bulk densities superior to 1 t/h, but lower densities increase these requirements.

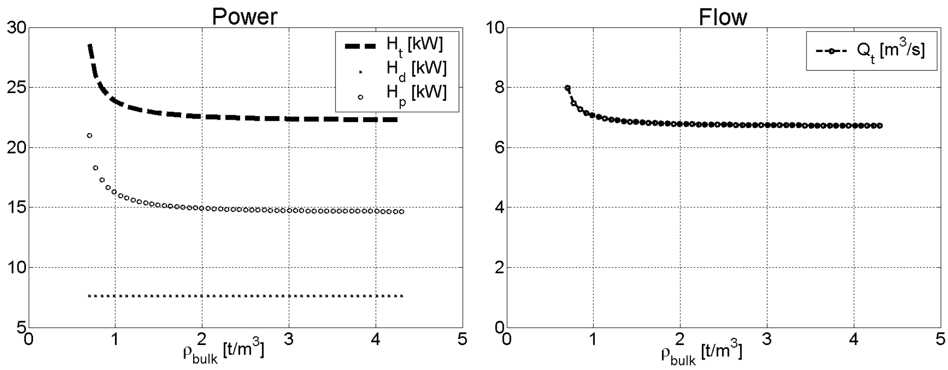

Figure 7.16: Power and Flow vs bulk material density

In the range $0.7 < \rho_{bulk}[t/m^3] < 4.3$ the flow has a variation of 19% with reference to the lower value. This is due to the supply pressure that changes in the same proportion. The pumping power is thus also affected.

Higher density materials allow for slightly lower flow and power consumption for fixed velocity, capacity and belt width.

Influence of Bulk Density on Temperature and Tensions

Tensions and temperature rise are not significantly affected by bulk density.

The variation in temperature rise due to bulk density is less than $1°C$ for $0.7 < \rho_{bulk}[t/m^3] < 4.3$.

Belt tensions are not affected by bulk material density.

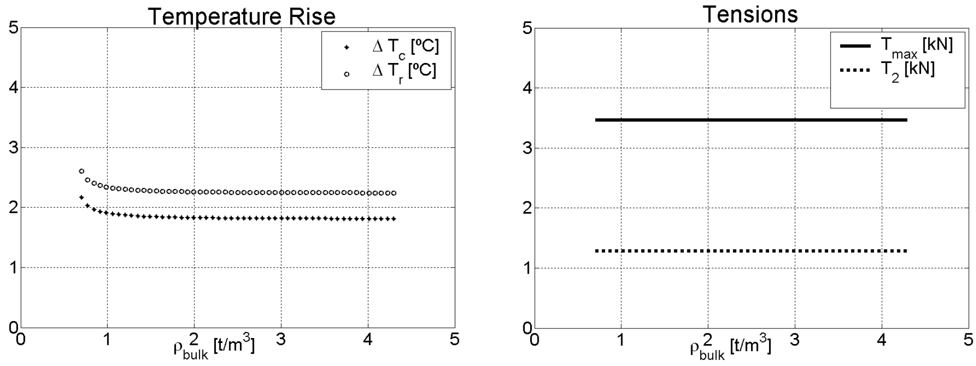

Figure 7.17: Temperature rise and belt tensions vs bulk material density

7.2.7 Influence of Conveying Angle

The natural conveying angle is a property of the bulk material. It specifies the maximum value that the conveying angle can achieve. It can be limited in the loading zone to have lower values.

Conveying angle has influence mainly on power, flow , and geometric parameters.

Influence of Conveying Angle on Power and Flow

Higher conveying angles increases both pumping power and flow.

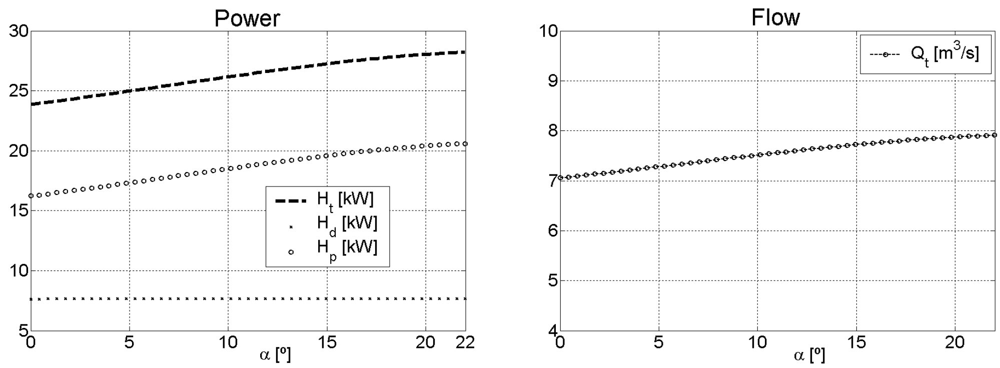

Figure 7.18: Power and flow vs conveying angle

As the conveying angle increases also the maximum load pressure. This will affect flow and supply pressure directly, and the pumping power is increased. The flow increases because it is directly dependent on the load pressure, and to keep a certain fluid thickness it must be higher.

A conveying angle $\alpha = 0$ is more advantageous in terms of pumping power and flow.

Influence of Conveying Angle on Temperature Rise and Belt Tensions

Temperature rise and belt tensions are not significantly affected by conveying angle.

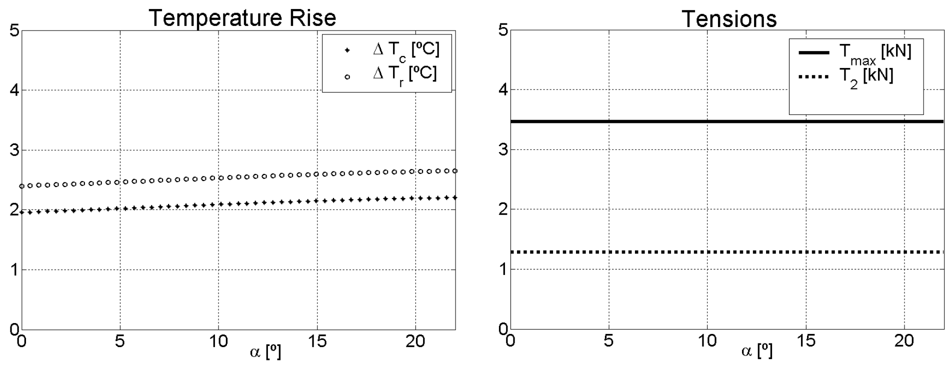

Figure 7.19: Temperature rise and belt tensions vs conveying angle

The conveying angle effect on temperature rise is low (less than $1°C$).

Due to the increase in load pressure the fluid thickness changes locally and this affect the drag force; but this effect is small. For tensions in the belt there is no noticeable change with conveying angle.

Influence of Conveying Angle on Geometric Parameters

Conveying angle has little influence on the support thickness. Its influence is more noticeable in the troughed radius.

An higher conveying angle allow to have a higher bulk area; the belt arc angle decreases. If the belt arc angle is near 180° the conveying angle can be

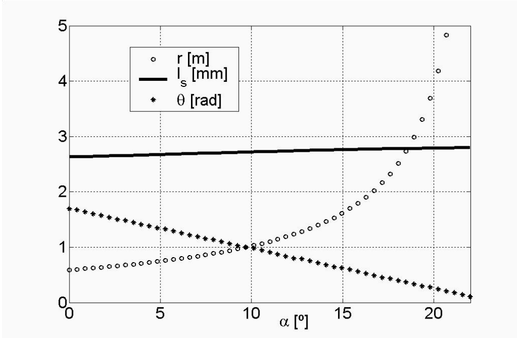

Figure 7.20: Support radius and thickness, belt arc angle vs conveying angle

increased to allow for more capacity.

The support thickness has a variation of 6% for $\alpha[^\circ] = 22$

7.2.8 Influence of Carrying Side Fluid Thickness

The pumping power, flow and temperature are highly dependent on the carrying side fluid thickness. Belt tensions are not so affected.

Influence of Carrying Side Fluid Thickness on Power and Flow

Pumping power and flow depend exponentially on the carrying side fluid thickness.

According to expression (4.9) the flow depends on the third power of the fluid thickness. This will affect also the pumping power.

The drive power changes due to the viscous drag force dependence on fluid thickness.

In the range $0.1 < h_c[mm] < 1.0$ the behavior of pumping power and flow with carrying side fluid thickness is strong. In relation to that the effects on drive power are not so noticeable, but change in opposition.

With reference on $h_c[mm] = 0.6$, for $h_c[mm] = 0.1$ the flow and the the pumping power have a variation of -91%, the drive power $+25\%$, and the total power -54%. For $h_c[mm] = 1.0$ the variation is $+324\%$ for pumping

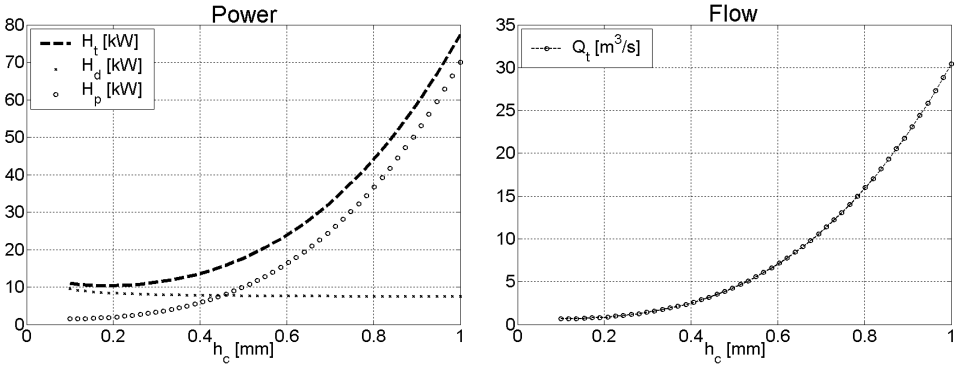

Figure 7.21: Power and flow vs carrying side fluid thickness

power and flow, -2% for drive power and $+322\%$ for the total power.

The minimum for the total power H_t is achieved not in one extreme of fluid thickness but for $h_c[mm] \approx 0.2$ having the value $H_t[kW] \approx 10$.

Influence of Carrying Side Fluid Thickness on Temperature Rise and Tensions

Tensions and temperature rise increase with smaller fluid thickness.

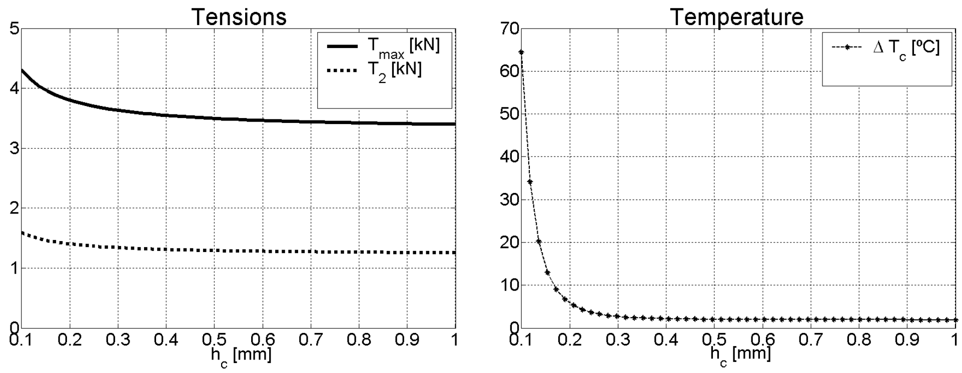

Figure 7.22: Temperature rise and tensions vs carrying side fluid thickness

Temperature rise becomes a problem for small fluid film thickness $h_c[mm] < 0.15$. The extreme value is $\triangle T_c[°C] = 64$. For $h_c[mm] > 0.3$ the temperature rise in the carrying side is lower than $3°C$.

For $h_c[mm] = 0.1$, due to higher drag force F_c, the take-up tension T_2 and the working tension T_{max} change +25%. For $h_c[mm] = 1.0$ the variation is around −2%.

7.2.9 Influence of Return Side Fluid Thickness

As for the carrying side, the return side fluid thickness has influence on pumping power, flow, temperature and tensions. The effects on pumping power and flow are reduced, while with temperature it is more accentuated.

Influence of Return Side Fluid Thickness on Power and Flow

The dependency of power requirements and flow on return side fluid thickness is not so strong as with carrying side fluid thickness.

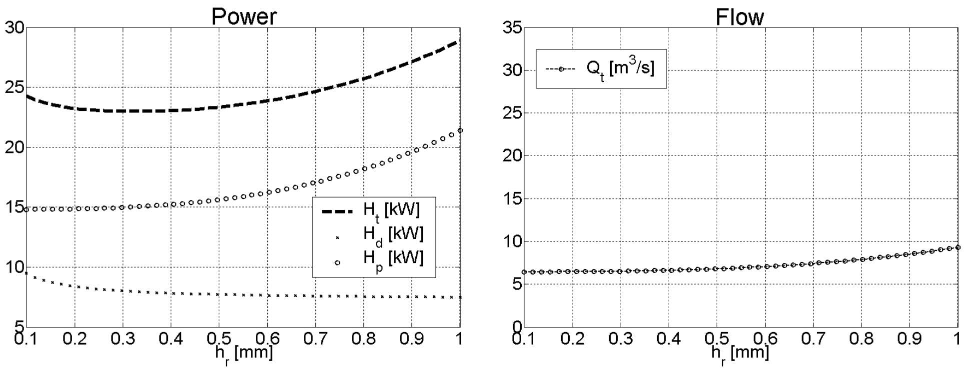

Figure 7.23: Power and flow vs return side fluid thickness

With reference on $h_c[mm] = 0.6$, for $h_c[mm] = 0.1$ the flow and the pumping power have a variation of −9%, the drive power +24%, and the total power −2%. For $h_c[mm] = 1.0$ the variation is +32% for pumping power and flow, +2% for drive power and +21% for the total power.

The minimum for the total power H_t is achieved in a bride range, $0.2 < h_c[mm] < 0.5$, with the value $H_t[kW] \approx 23$.

Influence of Return Side Fluid Thickness on Temperature Rise and Tensions

Temperature rise is critical for small return side fluid thickness.

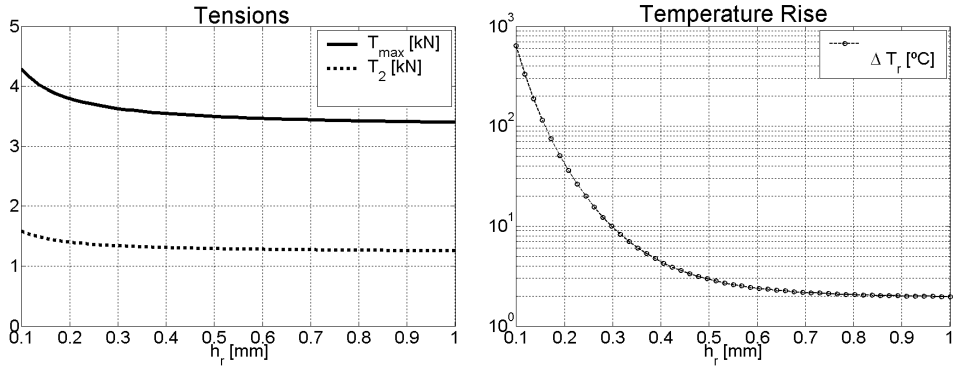

Figure 7.24: Temperature rise and tensions vs return side fluid thickness

The fluid temperature rise in the return side is more severe for small fluid thickness than in the return side. This is due to the low flow in the return side.

For $h_r[mm] = 0.1$ the temperature rise has a value of $\triangle T_r[°C] = 640(!)$, which would lead to belt destruction. This exquisitely high value result from the combination of high power dissipation due to the viscous drag force and a very small heat dissipation by convection, as the flow necessary to keep a fluid thickness of $h_r[mm] = 0.1$ in the return side is very small. For $h_r[mm] > 0.3$ the temperature rise is less than $10°C$.

For tensions, the results do not differ as much as for the carrying side. For $h_r[mm] = 0.1$, the take-up tension T_2 and the working tension T_{max} change $+24\%$. For $h_r[mm] = 1.0$ the variation is also around -2%.

7.2.10 Influence of Belt Width

Geometric parameters are affected by belt width. It has also influence on power, flow, tensions and temperature rise.

Influence of Belt Width on Power and Flow

Wider belts require less pumping power and flow but more drive power.

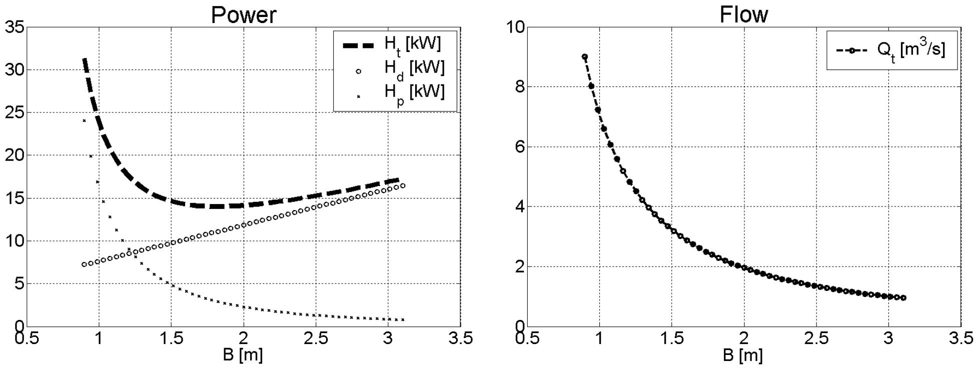

Figure 7.25: Power and flow vs belt width

As the belt gets wider, the required flow to maintain the fluid thickness is lower. Also a wider belt decreases the maximum load pressure, as the bulk material is more spread. With this the pumping power decreases also.

The drive power increase as a primary consequence of the scrapers resistance and the viscous drag force, which are proportional to the belt width. The scrapers resistance is the major contributor to the increase in drive power with increase in belt width; the relation between the scrapers resistance and the viscous drag force is of about 10.

The minimum value for the total power is $H_t[kW] \approx 14$ and it is achieved for $1.6 < B[m] < 1.8$.

For $B[m] = 1.6$ the flow is reduced to -60%.

Influence of Belt Width on Tensions and Temperature Rise

Wider belts increase tensions and have a modest effect on temperature rise.

The tensions on the belt are affected by the increase on the scrapers force and the viscous drag force in both sides. For $B[m] < 1.9$ the take-up tension is based on the rope friction law, and for $B[m] > 1.9$ to avoid negative tensions.

The temperature rise is directly proportional to the dissipated power and

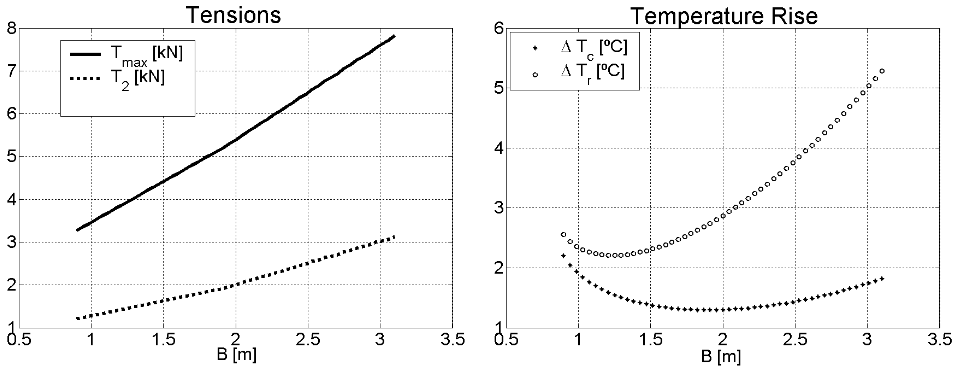

Figure 7.26: Tensions vs belt width

inversely to the flow. The dissipated power has to do with pressure drop since the orifice to the belt edge and the drag resistance. The combination of these factors lead to a nonlinear behaviour of the temperature rise for different belt widths.

In absolute values and for the range $0.9 < B[m] < 3.1$, $\triangle T_r$ changes $3°C$ and $\triangle T_c$ changes $1°C$.

Influence of Belt Width on Geometric Parameters

Wider belts require thicker and wider supports.

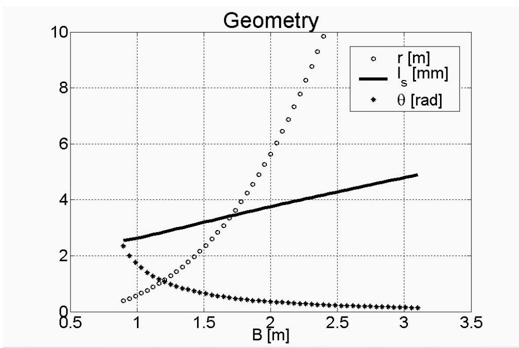

Figure 7.27: Support radius and thickness, belt arc vs belt width

A wider belt leads to smaller belt arcs and higher support radius.

The influence on support thickness is practically linear, but considerable. A linear regression is $l_s[mm] = 1.1 \times B[m] + 1.6$.

7.2.11 Influence of Carrying Side Pressure Ratio

The pressure ratio $\beta = p_{max}/p_s$ can be influenced by the load and/or supply pressures. Having a fixed load pressure the pressure ratio is decreased with increase in supply pressure.

The carrying side pressure ratio has influence on power, flow and temperature rise.

Influence of Carrying Side Pressure Ratio on Power and Flow

Smaller pressure ratios demand an increase in pumping power. Flow requirements are not affected.

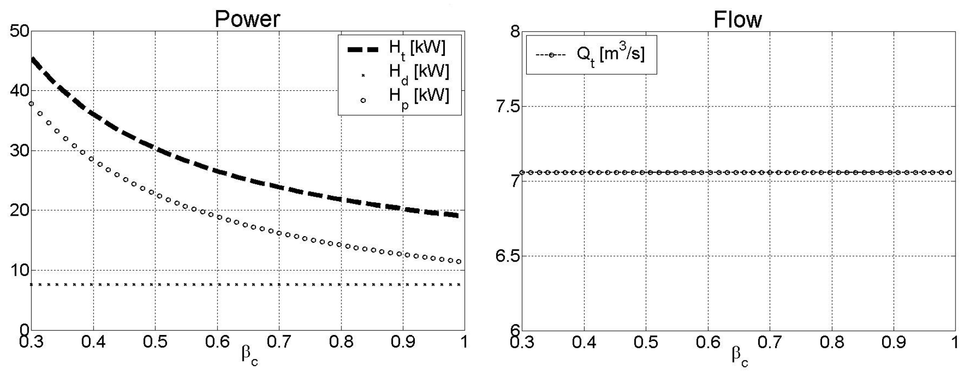

Figure 7.28: Power and flow vs carrying side pressure ratio

The pumping power depends on the pressure ratio. Lower pressure ratios increase pumping power. In relation to the actual $\beta = 0.7$, H_p can have an extreme reduction of -29% for $\beta = 0.99$, though the bearing will loose its response to overloads.

The required flow is not affected by the pressure ratio and remains constant at $Q_t[m^3/s] = 7.1$.

Influence of Carrying Side Pressure Ratio on Temperature Rise and Geometric Parameters

Lower pressure ratios demand thicker supports.

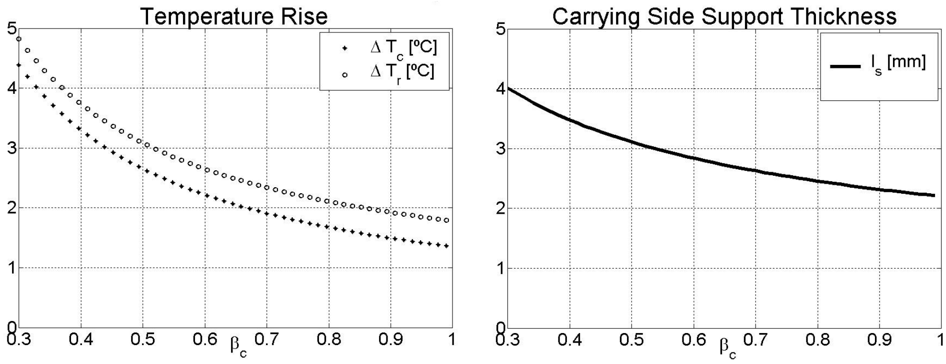

Figure 7.29: Support thickness and temperature rise vs carrying side pressure ratio

The lower the pressure ratio the higher the temperature rise, because the dissipated power in the orifice is considered to remain in the fluid.

The support thickness depends directly on the supply pressure; the behavior with $\beta_c = p_{max}/p_s$ is thus inverse. It can have a reduction of -16% for $\beta = 0.99$.

7.3 Comparison with Existent Air-Cushion Conveyors

In paper [24] the air-cushion conveyor performance is illustrated with references of existent applications in South Africa and Europe. The manufacturer is *Aerobelt C.C.*,a South African company. The information about the conveyors comprehend:

- Capacity $C[t/h]$
- Length $L[m]$
- Belt width $B[mm]$
- Bulk material density ρ_{bulk}
- Bulk material
- Drive motor power $H_{motor}[kW]$
- Flow $Q_{fan}[m^3/min]$
- Fan pressure $p_{fan}[mmH_20]$
- Fan drive power $H_{fd}[kW]$
- Inclination $\arctan(H/L)[°]$

The samples were chosen by their length, with preference for the longest.

Model Configuration

The model configuration for this comparison is the same as the reference configuration, with the difference on the tabulated parameters in table (7.5) and considering return side with moving mass $Q = 0.4 \times 21kg/m$, suggested from reference [10].

Drive Power

It is not possible to perform a fair comparison between the drive motor power of the applications with the drive power obtained by the air-cushion conveyor model. This because for short lengths the influence of accessories as belt cleaners is substantial compared with the distributed viscous drag force and idlers resistance. Such details were not available. Furthermore, the motor power is usually chosen with a considerable margin ($\sim +50\%$ of the required power).

Pumping Power, Flow and Supply Pressure

The supply working point (p_s, Q_t) is not given in the paper. It will be considered $p_s = p_{fan}$ and $Q_t = Q_{fan}$ to allow for some comparison. The tabulated results are relative to this assumption.

The model flow Q_t/L is greater or equal than Q_{fan}/L in the 5 cases, being closer to those with wider belts (case 4 & 5). This result is vicious because the fluid thickness of the model was chosen so that the flow would be similar ($h_c = h_r = 0.6mm$)!

The product $p_{fan} \times Q_{fan}$ is about 22 (case 1) to 3 (case 4 and 5) times less than the installed fan drive power H_{fd}. Even counting with a low efficiency, fan drives are chosen with power much above the required.

The pumping power of the model $H_p/L = p_s Q_t/L$ is from 1.2 to 4.8 times lower than the product $p_{fan} \times Q_{fan}/L$ of the studied cases. The model supply pressure p_s is 2.7 to 5.4 lower than the fan pressure p_{fan}. It would be favorable to know more details about the supply circuit to consider the influence of filters and losses in ducts. Factors as pressure ratio, conveying angle and support structure geometry have also considerable influence on the required fan pressure.

In reference [7], *Process fan and compressor selection*, typical values for fans and drives efficiency can be obtained. Filters efficiency depend on the type and size of filter and can be designed for a wide range of efficiency. Using reasonable values: considering fans with an efficiency of 83%, filters with 80% efficiency and motors with 95%, the real pumping power would be of about 60% more than the value H_p. With this the corrected power of the model H_p/η is from 1.3 times higher to 2.9 times lower than the references, with average at 1.6 times lower.

Parameter	**Symbol**	**Unit**	**1**	**2**	**3**	**4**	**5**	**Mod.**
Capacity	C	t/h	60	60	60	60	30	60
Bulk material	-	-	Salt	Wheat	Sand	Wood chips		-
Bulk density	ρ_{bulk}	t/m^3	1.10	0.50	1.60	0.23	0.23	1.00
Length	L	m	93	65	58	48	59	50
Belt width	B	m	0.40	0.40	0.40	0.90	0.60	0.40
Drive power	H_{motor}	kW	4.0	4.0	1.1	7.5	5.5	(1.9)
Incline	$\arctan(H/L)$	$°$	N.A.	N.A.	N.A.	25	15	0
Flow	Q_{fan}	m^3/s	0.18	0.12	0.08	0.17	0.17	0.19
Fan pressure	p_{fan}	Pa	1834	1471	1961	2942	2942	(543)
Fan drive power	H_{fd}	kW	7.5	2.5	3.7	1.5	1.5	-
Pump. power (1)	$p_{fan} \times Q_{fan}$	kW	0.33	0.18	0.16	0.50	0.50	(0.10)
Pump. power (2)	$p_{fan} \times Q_{fan}/L$	W/m	3.5	2.6	2.8	10.2	8.5	2.1
Flow per length	Q_{fan}/L	$lts/s/m$	1.9	1.8	1.4	3.8	2.9	3.8

Table 7.5: Comparison with existent air-cushion conveyors

The losses in ducts depend on the plenum geometry and were not considered yet. For an approximation made with a square duct of $0.25m$ side over a length of $125m$ with flow at $1.75m^3/s$, the pressure loss was of about $30Pa$ which is in the order of 1% of the usually required supply pressure and pumping power. It has not significant influence among the overall assumptions.

The cases with belt width equal to the model ($B = 0.4m$) have more similar results.

General Appreciation

The results on pumping power and supply pressure are below the ones in the studied cases. This comparison is not conclusive. Data is lacking on fluid thickness, fan working point, conveying angle, velocity, hydraulic circuit configuration, accessories and on the effective drive power. The comparison also depends on factors that are undetermined like fan and drives efficiency and losses in the supply system.

The carried comparison was useful to specify the fluid thickness at $h_c = h_r = 0.6mm$, so that flow and pumping power could be in the same magnitude.

7.4 Simulations With ANSYS

A model for the flow in the clearance was created with ANSYS. The model is the most simple possible. It consists in an area to whose limiting lines along length were applied non-slip boundary conditions and the other lines have pressure conditions: the maximum load pressure and the atmospheric pressure in relative values.

7.4.1 Results

For the configuration studied in this chapter (with $h_c[mm] = 0.6$ and $B[m] = 1$) the maximum load pressure is $p_{max}[Pa] = 1609.2$ resulting in a flow of $Q_{c(model)}[lt/s/m] = 6.437$.

The solution was set to finish with velocity convergence of $10^{-3}m/s$ and pressure convergence of $10^{-2}Pa$. The number of necessary iterations to converge was 63 for the laminar flow and 61 for the turbulent flow.

Laminar Flow

Assuming laminar flow the resulting outlet velocity profile is as in figure (7.30). In this figure the pressure profile along belt width is also plotted, being linear.

The integral of the velocity profile over the fluid thickness gave $Q_{c(ANSYS)}[lt/s/m] = 6.216$. The comparison translates into an error of +3.6% related to ANSYS results. Air-properties are the same in both cases. The Reynolds number for the ANSYS result is $Re = 311$.

With low Reynolds number ($Re < 2300$) the laminar flow assumption is considered to produce satisfactory results.

Turbulent Flow

Specifying a turbulent flow the difference is more salient, with $Q_{c(ANSYS)}[lt/s/m] = 4.026$. With this reference the model error is +60%. The Reynolds number for this last ANSYS result is $Re = 201$.

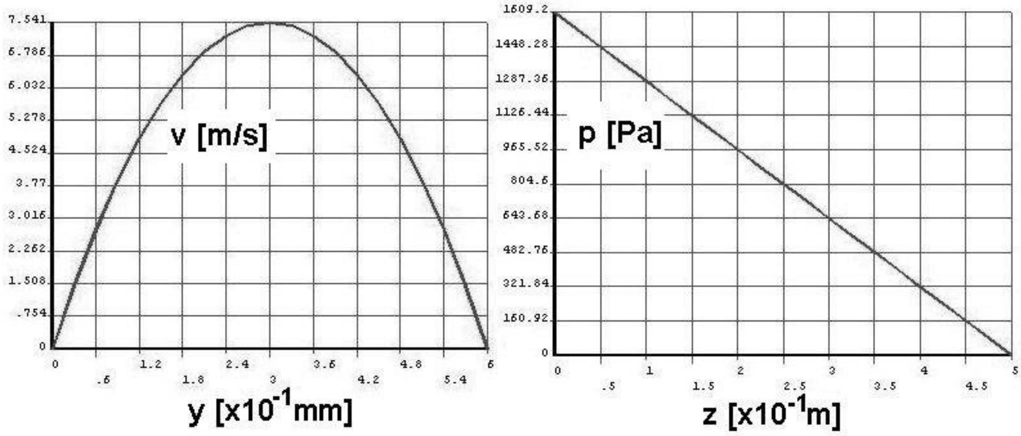

Figure 7.30: Velocity and pressure profile in a laminar flow ANSYS simulation

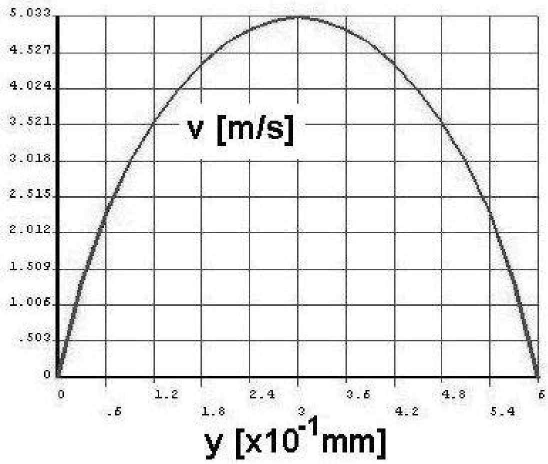

Figure 7.31: Velocity profile in a turbulent flow ANSYS simulation

Usually algorithms to solve turbulent flow produce results with a considerable margin for error. In the case of low Reynolds number, considering turbulent flow is an error in itself, because the turbulence models predict low values of effective viscosity.

Synthesis

A low Reynolds number in the outlet is favorable for the assumption of laminar flow. Comparison with ANSYS simulations revealed that the results for flow diverge in about +4%.

7.5 Evaluation of Variable Fluid Thickness Effects

The dependence of fluid thickness on the pressure differential can be reflected on the flow.

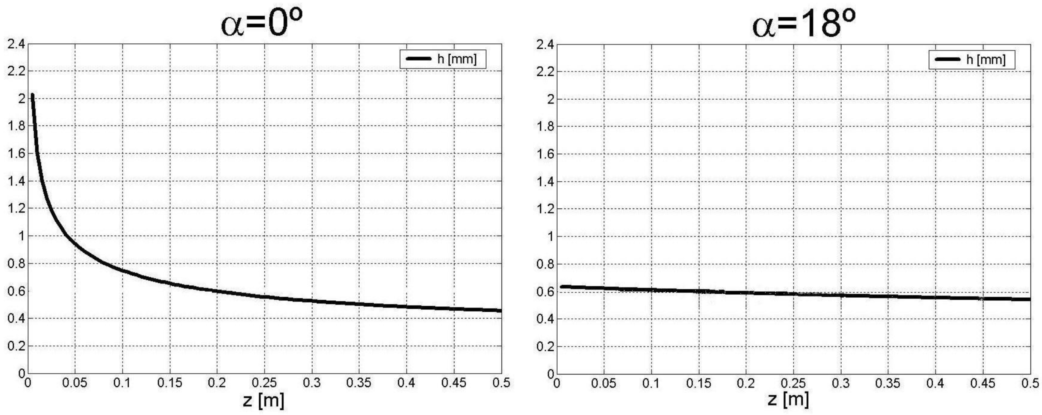

Figure 7.32: Theoretical fluid thickness vs position along width

Figure 7.32 presents the theoretical value of fluid thickness along belt width for conveying angle $\alpha = 0°$ and $\alpha = 18°$.With $\alpha = 0°$ the fluid thickness is theoretically infinite in the center, where the pressure differential is $\partial p/\partial z = 0$. This result is unreal, but it predicts that the fluid is thicker in the trough center. With $\alpha = 18°$ (natural conveying angle of coal) the pressure differential is more linear and also the fluid thickness profile.

For flow purposes the clearance can be seen as a series of hydraulic resistances with lengths δz and heights $h(z)$. The total resistance is the integral $R = R_0 h_0^3 \int \frac{1}{h^3(z)} dz$, where R_0 is the resistance calculated with constant $h = h_0$.

The integral $\int \frac{h_0^3}{h^3(z)} dz \approx 0.8$. If a conveying angle $\alpha = 18$ is considered the fluid thickness profile is different and the integral is ~ 0.9.

The local fluid thickness is thus a factor to take in consideration for flow calculations. The error can be of about -20% of the required value.

7.6 Efficiency and Correction Factors

After computing the pre-design parameters the following corrections should be applied, to better estimate power requirements and geometry.

Required Flow

$$Q_{fan} \approx \frac{Q_t}{\eta_\alpha} \tag{7.1}$$

η_α is the variable fluid thickness factor:

$$\eta_\alpha = h_0^3 \int \frac{1}{h^3(z)} dz \tag{7.2}$$

The value η_α can be obtained with the MATLAB command:

```
(hc/mean(hz))^3
```

Fan Pressure

$$p_{fan} \approx \frac{p_s}{\eta_{supply}} \tag{7.3}$$

η_{supply} - supply circuit efficiency (including filters)

Required Fan Drive Power

$$H_{fd} \approx \frac{H_p}{\eta_\alpha \eta_{fan} \eta_{motor} \eta_{supply}} \tag{7.4}$$

η_{motor} - drive efficiency
η_{fan} - fan efficiency

Required Drive Motor Power

$$H_{dm} \approx \frac{H_d}{\eta_{motor}\eta_{reducer}\eta_{slip}} \tag{7.5}$$

η_{slip} - coupling efficiency
η_{motor} - motor efficiency
$\eta_{reducer}$ - reducer efficiency

Orifice Diameter

$$d_{orif} \approx d\sqrt{\frac{1}{\eta_\alpha}} \tag{7.6}$$

Support Radius

$$r_t \approx r + t_{belt} \tag{7.7}$$

Chapter 8

Service Conditions

In this chapter the performance of the air-cushion conveyor with the reference configuration and results of the last chapter will be analyzed with respect to changes in ambient temperature, capacity and supply pressure. During this analysis the geometry of the conveyor is kept.

8.1 Ambient Temperature Variations

Ambient temperature have effect on air viscosity and density. During the conveyor service temperature variations have some influence on the overall performance.

8.1.1 Effect on Flow and Power

With relation to the reference temperature $T[^\circ] = 20$, in the range $-20 < T[^\circ] < 60$, the flow and the pumping power changes about $\pm 6\%$, and the drive power $\pm 1\%$. The total power increases with higher temperatures.

8.1.2 Effect on Fluid Thickness

The fluid thickness increases with temperature and has a variation of $\pm 5\%$ in the range of temperatures considered.

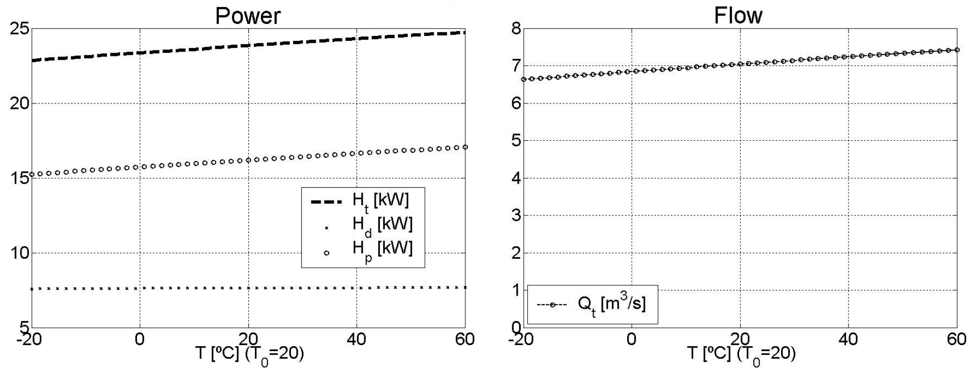

Figure 8.1: Power and flow vs ambient temperature

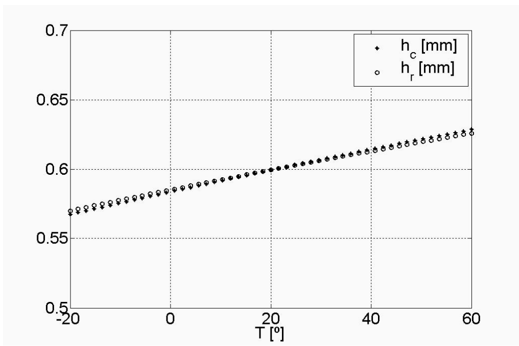

Figure 8.2: Fluid thickness vs ambient temperature

8.1.3 Effect on Temperature Rise and Belt Tensions

Tensions in the belt are not significantly affected by temperature. The working tension change 1% in the range of temperatures considered.

The temperature rise is proportional to the ambient temperature, but the variation is also not significant; for $-20 < T[^\circ] < 60$ the range is less than $1^\circ C$. With this result comes also the conclusion that the temperature rise in the fluid does not have an important effect on belt tensions.

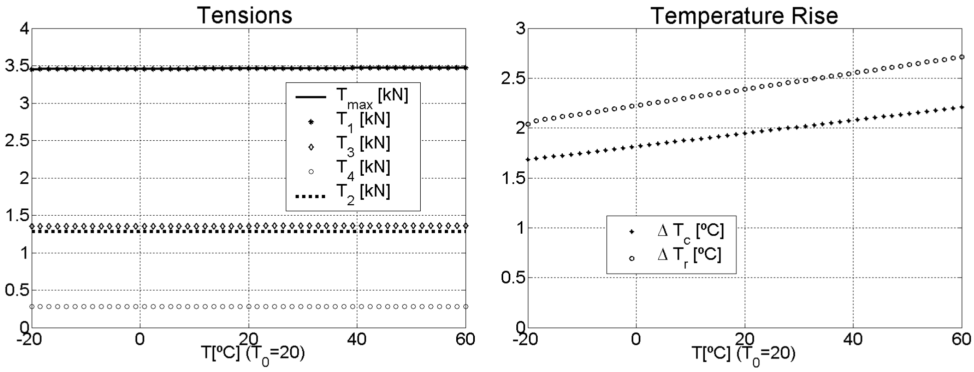

Figure 8.3: Temperature rise and belt tensions vs ambient temperature

8.2 Supply Pressure Variations

The supply pressure has effect mainly on flow, power, tensions, temperature, and fluid thickness. The take-up tension is kept constant during the analysis.

8.2.1 Effects on Fluid Thickness

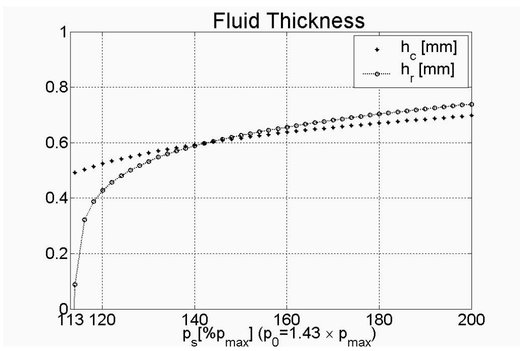

Figure 8.4: Fluid thickness vs supply pressure

With p_s changing the supply pressure in the return side, p_{sret} will change proportionally. The pressure ratio $\beta = p_{load}/p_s$ is higher in the return side; with $p_s \rightarrow 114\% p_{max}$, $p_{sret} \rightarrow ps_{maxret}$ and the fluid thickness $h_r \rightarrow 0$.

8.2.2 Effects on Flow and Power

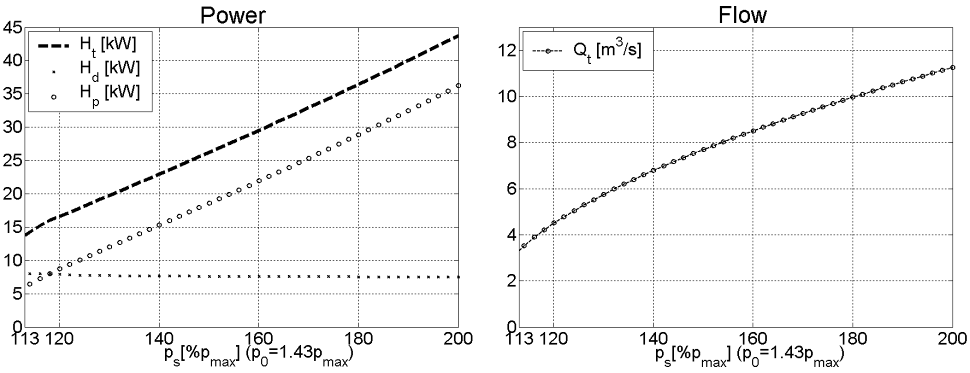

Figure 8.5: Power and flow vs supply pressure

While the drive power is practically constant, the pumping power changes by the double effect of flow and supply pressure.

8.2.3 Effects on Temperature Rise and Belt Tensions

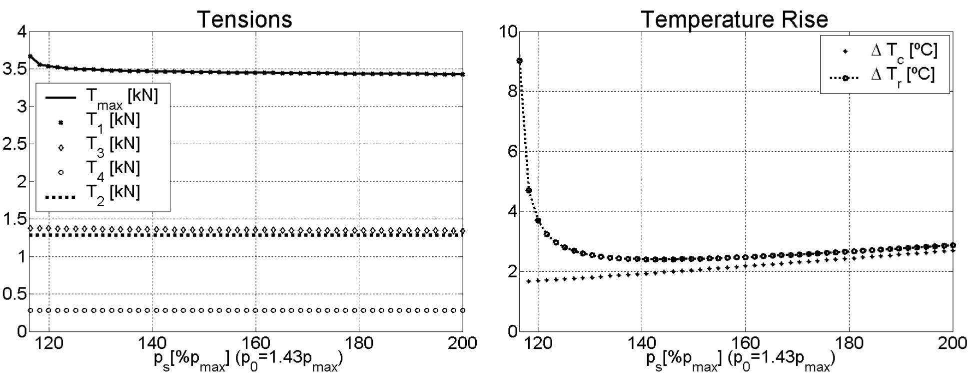

Figure 8.6: Temperature rise and belt tensions vs supply pressure

Temperature rise in the carrying side may become a problem for $ps < 115\% p_{max}$.

The working tension T_{max} increases also for smaller supply pressure as a result of decrease in fluid thickness, therefore increase in drag force resistance.

8.3 Changing Capacity

The capacity can be increased or decreased with belt velocity and conveying angle.

8.3.1 Changing Capacity with Belt Velocity

It is common to increase the belt velocity to increase capacity, having a constant bulk area. The relation of capacity with velocity is linear. the

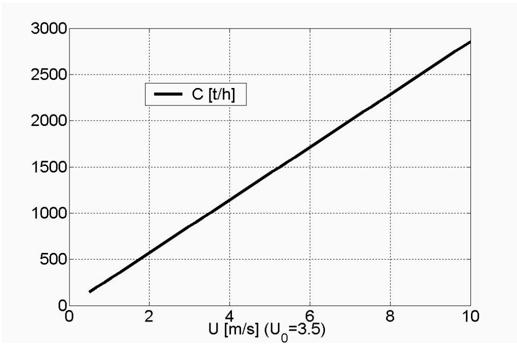

Figure 8.7: Capacity vs velocity

linear regression of the curve in graphic (8.3.1) is $C[t/h] = 290 \times U[m/s]$.

Effects on Temperature Rise and Belt Tensions

For higher velocities the take-up tension T_2 must be increased. For $U[m/s] < 2.6$, T_2 is determined to avoid compressible tensions, specifically to increase T_4, the tension in the tail pulley. For $U[m/s] > 2.6$, T_2 is specified by the rope friction law.

The working tension $T_{max} = T_1$, the tight side tension in the drive pulley. It increases also with velocity, decreasing the safety factor. Though, for $U[m/s] = 10$, the safety factor is still $sf = 21$ for the PN315/2 belt!

The temperature rise in the return side is more affected by velocity than in the carrying side. The dissipated power due to the viscous drag resistance is proportional to the square of the velocity. The range of variation is below $6°C$ for the return side and around $2°C$ for the carrying side.

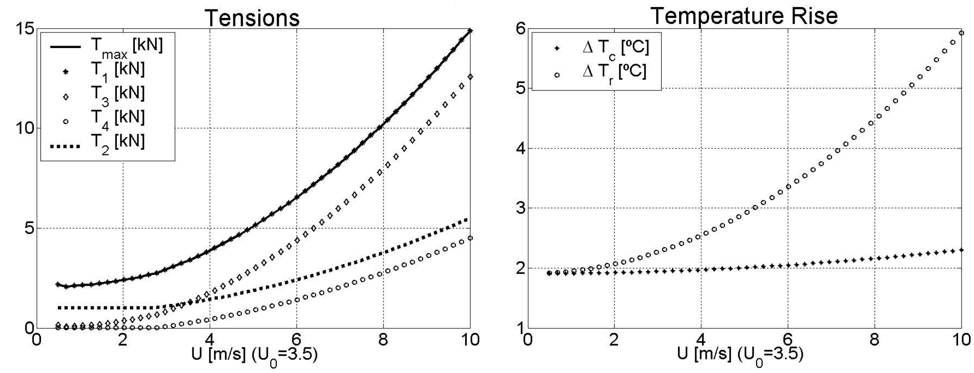

Figure 8.8: Temperature rise and belt tensions vs velocity

Effects on Power and Flow

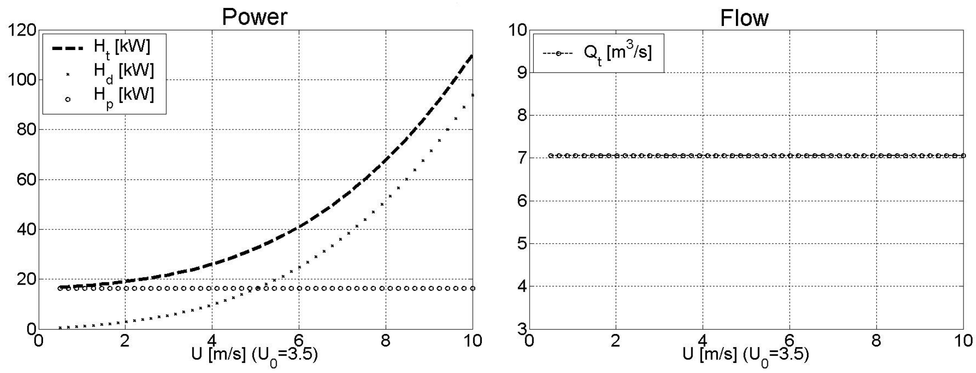

Figure 8.9: Power and flow vs velocity

The flow is constant ($Q_t[m^3/s] \approx 7$), as the load pressure is the same.

With constant flow the pumping power is also constant. The drive power by the other hand has a quadratic behaviour which reflects on the total power.

8.3.2 Changing Capacity with Conveying Angle

It is also possible to increase the capacity with conveying angle. This have more limitations than with velocity. The bearing performance will be negatively affected.

This is useful only when belt wear is an important factor. It depends on the square of belt velocity.

The linear regression is $C[t/h] = 34 \times \alpha[°] + 1000$.

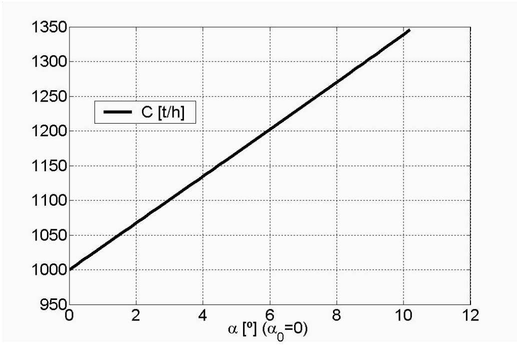

Figure 8.10: Capacity vs conveying angle

Effects on Fluid Thickness

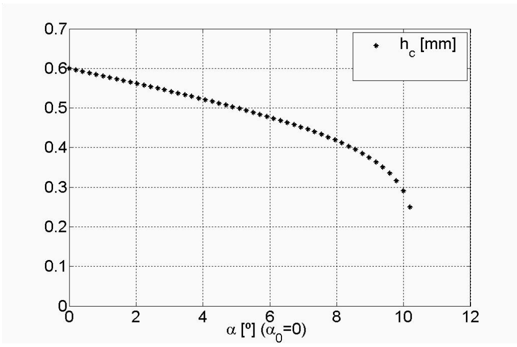

Figure 8.11: Carrying side fluid thickness vs conveying angle

Increasing the conveying angle will decrease the fluid film thickness h_c, due to the increase in load pressure. As $\alpha[°] \to 10.3$, $h_c \to 0$ and the load pressure $p_{max} \to p_s$.

Considering the maximum capacity that can be achieved changing the conveying angle, $C[t/h] \approx 1350$, the initial overload ratio $W/W_0 = 1.50$ is quite different from the capacity ratio $C/C_0 = 1.35$, that is in practice the maximum that can be achieved.

Effects on Power and Flow

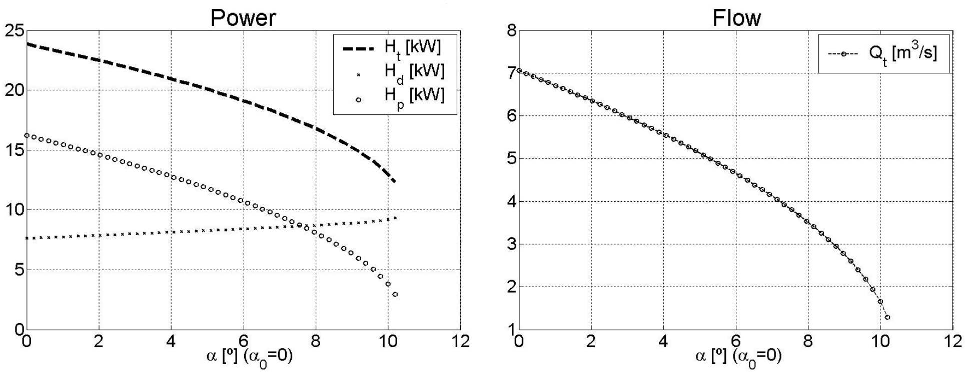

Figure 8.12: Power and Flow vs conveying angle

Having the supply pressure constant, as the fluid thickness becomes thinner the flow is reduced and so the pumping power. The drive power increases slightly, but the total power decreases.

Effects on Temperature Rise and Belt Tensions

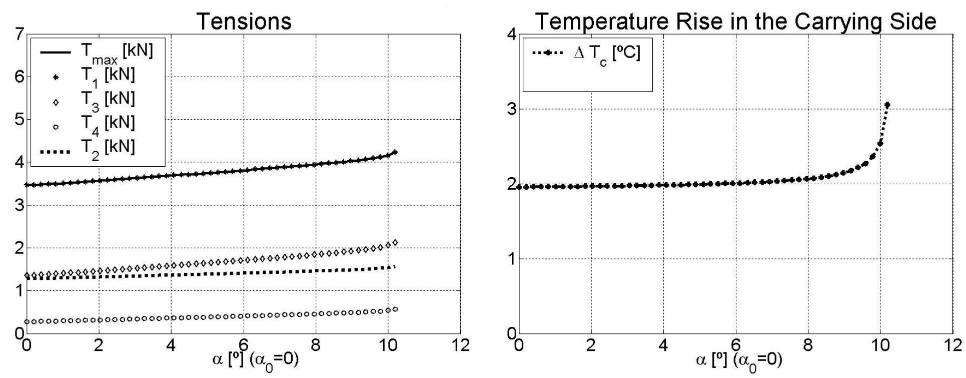

Figure 8.13: Temperature rise and belt tensions vs conveying angle

Belt tensions get also higher with increase in capacity using conveying angle. The force to accelerate the bulk material increases proportionally to the capacity, and the viscous drag force is increased as a consequence of lower fluid thickness.

In the extreme value, when $\alpha[°] \to 10.3$ the temperature in the carrying side $\triangle T_c \to \infty$ because the flow $Q_t \to 0$.

Chapter 9

Dynamics

9.1 Dynamic Model

9.1.1 Assumptions

Reference [7] suggests for hydrostatic bearings a dynamic model as in figure (9.1) with the assumption of fluid incompressibility.

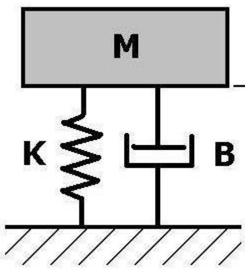

Figure 9.1: Air-bearing dynamic model

Using this model for the air-supported belt conveyor is possible with the following assumptions:

Fluid Incompressibility: this assumption is reasonable since the pressures involved are low, and having the orifices a small diameter the dynamics is little influenced by the air volume in the ducts.

Negligible Fluid Inertia: For small variations of the fluid thickness the changes in air velocity out of the orifices is small and also the influence on the bearing dynamics. This assumption requires small disturbance forces.

Rigid Load Mass: disregards belt and bulk material flexibility and considers the mass as being concentrated. Flexibility of the load is substantial and for wider, lower thickness belts this is a weak assumption.

9.1.2 Parameters

Mass

The mass is calculated as:

$$M = \frac{CD_x}{U} \tag{9.1}$$

C - capacity
D_x - pad length
U - belt velocity

Stiffness

The expression for stiffness comes from the static response of the bearing to loads and in case of hydrostatic bearings with orifices as flow restrictors, the stiffness is:

$$K = 3\frac{W_0}{h_0}\frac{1-\beta}{1-\beta/2} \tag{9.2}$$

$W_0 = M \times g$ - load in the initial configuration
h_0 - initial fluid thickness
β - pressure ratio

Damping

The damping element B is the squeeze coefficient of the bearing:

$$B = \frac{\mu_{air} D_x b^3}{4h_0^3} \tag{9.3}$$

μ_{air} - air viscosity
D_x - pad length
b - pad width
h_0 - fluid thickness in reference configuration

9.1.3 Transfer Function

The transfer function for this model represents a second order system:

$$\frac{Y(s)}{F(s)} = G(s) = \frac{1}{Ms^2 + Bs + K} \tag{9.4}$$

9.1.4 Implementation with Simulink

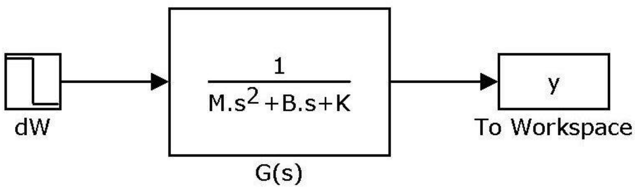

Figure 9.2: Simulink implementation

The transfer function $G(s)$ was implemented in MATLAB/Simulink. The input dW is the load disturbance and the output y the displacement.

Parameters	**Units**	**h=0.4mm**	**h=0.6mm**	**h=0.8mm**
K	$\times 10^6 N/m$	2.69	1.80	1.35
B	$\times 10^3 Ns/m$	43.8	13.0	5.47
ω_n	Hz	–	23.9	20.7
ξ	–	> 1	0.54	0.26
t_s	ms	58	39	107
Overshoot	%	–	12.9	41.7

Table 9.1: Model Parameters for different fluid thickness

9.2 Simulation

The expressions for the parameters were implemented in a m-file (AC_DynPar.m), in which all the variables should be specified, and which contains also the callings for the simulation.

9.2.1 Effects of fluid thickness

The results were obtained for three different fluid thickness. The system mass is $M[kg] = 79.4$.

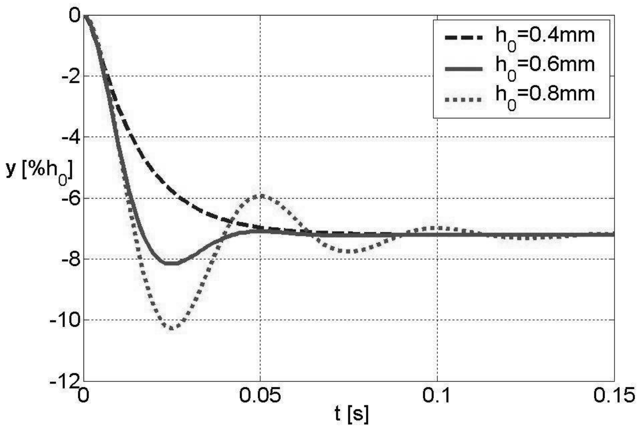

Figure 9.3: Response for a +10 % of nominal load step

Parameters	**Units**	$\beta = 0.3$	$\beta = 0.5$	$\beta = 0.7$	$\beta = 0.9$
K	$\times 10^6 N/m$	3.20	2.59	1.79	0.71
ω_n	Hz	32.0	28.8	23.9	15.0
ξ	$-$	0.41	0.45	0.54	0.87
t_s	ms	42	46	39	46
Overshoot	%	24.6	20.3	13.1	0.4

Table 9.2: Model Parameters for several pressure ratios

Analysis

The transfer function step response shape depends strongly on the fluid thickness. High values for fluid thickness make the system more oscillatory. Lower values make the system behaviour resemble first order systems, with damping values $\xi > 1$ and no overshoots.

9.2.2 Effects of pressure ratio

The effects of pressure ratio in the bearing performance is evaluated having a constant fluid thickness $h_0[mm] = 0.6$ and the squeeze coefficient $B[Ns/m] = 1.30 \times 10^4$. The equivalent mass is $M[kg] = 79.4$.

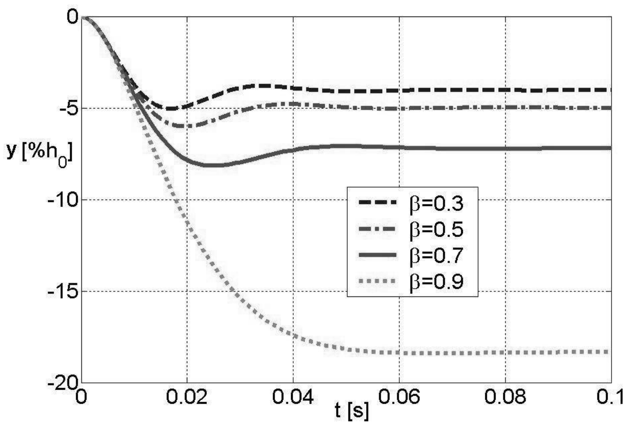

Figure 9.4: Response for a +10 % of nominal load step for different pressure ratios

Analysis

The pressure ratio has major influence in the settling point but also in the overshoot. Lower pressure ratios produce more overshoot, but the settling point is lower in absolute values. This behaviour is due to the increase in static stiffness as pressure ratios decrease.

9.3 Synthesis

In order to maintain the fluid thickness robust to disturbances the smallest fluid thickness is desirable.

A low pressure ratio is favorable to the settling point of the air-bearing, but it increases the overshoot. If the pressure ratio is high the settling point also, and the bearing performance is compromised.

At the orifice the inertia is not negligible and it is inversely proportional to the pressure ratio. Also the fluid thickness is locally high due to a low pressure differential in the belt width direction. Combining a large fluid thickness with low pressure ratio causes a bearing with low damping. It is therefore not reasonable to decrease too much the pressure ratio.

In the range of studied fluid thickness ($0.4 - 0.8mm$, $\beta = 0.7$) and pressure ratios($0.3 - 0.9$, $h = 0.6mm$) the system is stable.

With the assumptions made the lowest fluid thickness, associated with a reasonable pressure ratio is the best for performance in general.The used configuration is acceptable, $\beta = 0.7$ and $h = 0.6mm$, having about 13% overshoot and a settling point that is -8% of the static fluid thickness for a load disturbance of +10% the nominal load.

The assumption that considers the belt and load as a rigid body causes concern. The results of this section should be held in a qualitative scope.